Infrasound detection by laser diode self-mixing interferometry

Chengwei Li (李成伟)[1], Zhen Huang (黄 贞)[1,2*], and Xiaogang Sun (孙晓刚)[1]

[1]*School of Electrical Engineering and Automation, Harbin Institute of Technology, Harbin 150001, China*

[2]*School of Physical Science and Technology, Zhanjiang Normal University, Zhanjiang 524048, China*

[*]*Corresponding author: zzhuangzhen@163.com*

Received May 24, 2012; accepted September 4, 2012; posted online December 25, 2012

An alternative technique for infrasound detection based on the self-mixing (SM) interference of a laser diode is described. The principle involved is the dependence of the power emitted by the laser diode on infrasound-induced membrane vibration. The Fourier transform and fringe-counting methods are used to analyze the self-mixing signal. Infrasound signals are experimentally measured from 2 to 20 Hz with a resolution of 0.25, and the results well agree with the theoretical ones.

OCIS codes: 120.7280, 230.1040, 280.3420.

doi: 10.3788/COL201311.021201.

The nominal range of human hearing extends from approximately 20 Hz to 20 kHz. Inaudible sound waves with frequencies below 20 Hz are termed infrasound. These waves can be caused by many natural and anthropogenic sources, such as volcanic eruptions, earthquakes, typhoon, nuclear explosions, spacecraft, and so on[1]. Renewed interest in the detection of infrasound energy in the atmosphere appeared with the creation of the Comprehensive Nuclear-Test-Ban Treaty Organization[2]. A worldwide network of 60 infrasound stations is being established to help monitor compliance with the treaty[3]. Various non-contact, direct-sensing techniques exist, including laser-based interferometric or time-of-flight, capacitive, inductive, optical, and eddy-current (EC) sensing methods[4,5].

Infrasound detection using traditional sensors is based on piezoelectric principles[6]. Bruel and Kjaer market a low-noise microphone (type 4193) that responds at frequencies as low as 0.05 Hz and has impressive noise properties. The optical fiber infrasound sensor (OFIS) is an innovative device comprising two fibers (typically extending from 100 to 1 000 m) connected as a Michelson, Mach–Zehnder, or equivalent interferometer. Considering that the OFIS is longer than the distance over which wind-induced pressure changes are coherent, the effects of wind noise on infrasound detection is reduced, and the signal-to-noise ratio (SNR) is increased over a wide bandwidth[6,7]. These sensors enable accurate measurements but require many optical components, which make these sensors expensive to install and maintain. Eddy-current (EC) sensors that can perform well in water, are stable with temperature and relatively inexpensive, and have a small form. The EC infrasound sensor reported by Donskoy *et al.*[4] can detect acoustic signals below 1 Hz at displacement levels of fractions of nanometers. However, when using multiple probes, EC probes interact if mounted sufficiently close to one another.

Another alternative technique based on the self-mixing (SM) effect in a laser diode (LD) is presented in this letter. This method has been widely investigated over the last decades particularly for displacement measurements[8−11]. A self-mixing (SM) sensing scheme is advantageous because it does not require an optical interferometer external to the source and an external photo-detector. The laser itself is also used both as a source and a detector, resulting in a very simple and compact setup[12]. In this letter, we provide evidence that the laser SM effect can be applied in infrasound detection. Experimental results show that the proposed method can measure infrasound signals from 2 to 20 Hz with a frequency resolution of 0.25 Hz.

In the laser SM effect, a fraction of the light backreflected or backscattered by a target retraces the emission beam path into the laser cavity, inducing a modulation of both the amplitude and the frequency of the lasing field[8]. This phenomenon can be directly detected by a monitor photodiode (PD). According to Groot *et al.*, the laser SM effect can be easily elucidated by exploiting a three-mirror model[13]. In a more detailed analysis, the power emitted by the LD can be written as[14−16]

$$P(t) = P_0\{1 + m\cos[\omega_{\rm F}(t)\tau_{\rm ext}(t)]\}, \quad (1)$$

where P_0 is the power emitted by the unperturbed LD, m is a modulation index, $\omega_{\rm F}(t)$ is the angular oscillation frequency in case of feedback, and $\tau_{\rm ext}(t) = 2L_{\rm ext}/c$ is the round-trip propagation time in the external cavity.

Angular oscillation frequency in case of feedback can be calculated from the unperturbed oscillation angular frequency ω_0 by[17]

$$\omega_{\rm F}(t) + \frac{C}{\tau_{\rm ext}(t)}\sin[\omega_{\rm F}(t)\tau_{\rm ext}(t) + \arctan\alpha] = \omega_0, \quad (2)$$

where α is the LD linewidth enhancement factor and C is the feedback parameter.

C is highly significant because it discriminates among different feedback regimes. In the moderate feedback level ($1 < C < 4.6$), the SM signal exhibits hysteresis and the fringe shapes become sawtooth-like[18].

Figure 1 represents the sawtooth-like modulation of a simulated SM signal for a target excitation frequency of 9.75 Hz and a target excitation amplitude of $4\times(\lambda/2)$ with $C = 1.5$. D represents the sinusoidal displacement of the target versus time, and ΔP represents the

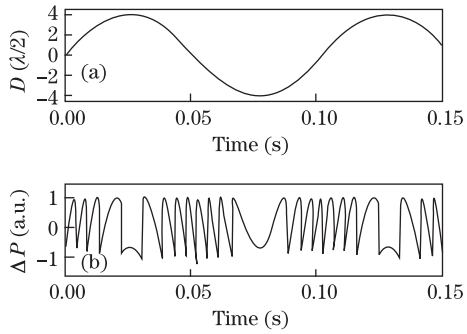

Fig. 1. Optical output power variation caused by a sinusoidal motion of the target, (a) simulated displacement of the target, and (b) stimulated optical output power of a LD focused on this moving target.

difference in the output optical power with and without feedback versus time. Each fringe period of interferences relates to a target displacement of a half-wavelength ($\lambda/2$), corresponding to a phase-shift of 2π.

$$|2\pi\omega_{\rm F}\Delta\tau_{\rm ext}| = 2\pi \Longleftrightarrow \Delta L_{\rm ext} = \lambda/2. \tag{3}$$

Therefore, the target displacement is easily recovered in steps of $\lambda/2$ without ambiguity through fringe counting[17]. Assuming that the frequency and amplitude of the target vibration are f_0 and A_0, respectively, the distance between the membrane surface and LD ($L_{\rm ext}$) can be expressed as

$$L_{\rm ext} = L_0 + A_0\sin(2\pi f_0 t + \varphi), \tag{4}$$

where φ is the initial phase and L_0 is the initial distance between the membrane surface and LD.

When N swings are determined for a motion in one given direction, the target vibrating amplitude is expressed by

$$A_0 = N\frac{\lambda}{2}. \tag{5}$$

The target vibrating frequency can be obtained from the demodulated displacement waveform. However, correct demodulation of the target displacement waveforms requires a relatively complex process[19,20]. To obtain the vibration frequency of the target more accurately and quickly, the Fourier transform (FT) method can be used. The theory of this method has been reported by Dai *et al.*[21] and can be summarized as follows.

By combining Eqs. (1) and (4), the power emitted by the LD can be written as

$$P = P_0\{1 + K\cos[\phi_0 + a\sin(2\pi f_0 t + \varphi)]\}, \tag{6}$$

where $\phi_0 = 4\pi L_0/\lambda$ and $a = 4\pi A_0/\lambda$.

By expanding Eq. (6) into a trigonometric series, the FT of the expanded form can be written as

$$\begin{aligned} F(f) = {} & F_0\delta(f) + m\cos\phi_0 {\rm e}^{-{\rm j}2n\varphi} \\ & \cdot\Big[\sum_{n=1}^{\infty} J_{2n}(a)\delta(f-2nf_0)\Big] + {\rm j}m\sin\phi_0 {\rm e}^{-{\rm j}(2n+1)\varphi} \\ & \cdot\Big\{\sum_{n=0}^{\infty} J_{2n+1}(a)\delta[f-(2n+1)f_0]\Big\}, \end{aligned} \tag{7}$$

where F_0 is the amplitude of a direct component, $\delta(f)$ is the impulse function, and f is its argument of frequency. $J_{2n}(a)$ and $J_{2n+1}(a)$ are even and odd order Bessel functions of the first kind with argument a, respectively.

Thus, the frequency spectrum of the SM signal is composed of f_0 and its harmonic components[21,22]. The corresponding Fourier spectrum of the SM signal in Fig. 1 is shown in Fig. 2. The spectrum exhibits a harmonic structure where a peak component exists at the fundamental vibration frequency in addition to many harmonic components[22]. The strongest peak (at 214.5 Hz) is approximately 22 times higher than the vibration frequency.

The feasibility of using a SM sensor in infrasound detection is demonstrated with the setup shown in Fig. 3. As the incident infrasound wave is broadcasting, the membrane vibrates and the vibration frequency is equal to that produced by the sound-field pressure. The membrane vibrates at the same frequency as that of the infrasound wave and changes its position relative to the LD. Assuming that the frequency and amplitude of the vibrating membrane are f_0 and A_0, respectively, the infrasound pressure can be described as[23]

$$p = \frac{8A_0T}{a_{\rm m}^2}, \tag{8}$$

where A_0 is the vibrating amplitude of the circuit membrane, $a_{\rm m}$ is the radius of the membrane, and T is the maximum tension of the membrane.

The infrasound pressure level (SPL) can be described as

$${\rm SPL} = 20{\rm lg}\frac{p}{p_{\rm ref}}, \tag{9}$$

where $p_{\rm ref} = 2\times10^{-5}$ Pa.

By combining Eqs. (5), (8), and (9), the relationship between the fringe number N and SPL can be expressed as

$${\rm SPL} = 20{\rm lg}\frac{4NT}{a_{\rm m}^2 p_{\rm ref}}. \tag{10}$$

SPL is proportional to lg(N). The number of fringes of SM signal changes with the SPL of the infrasound.

The validity of this method is experimentally confirmed with the setup shown in Fig. 4. A sinusoidal voltage from a signal generator is applied to the loudspeaker to form analog infrasound signals. A circular aluminum film is used as the vibrating diaphragm to provide sufficient light backreflected into the LD optical cavity. A commercial single-mode LD (QL65D5SA)

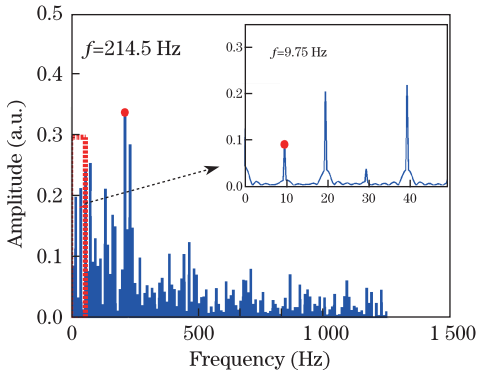

Fig. 2. Fourier spectrum of the simulated SM signal.

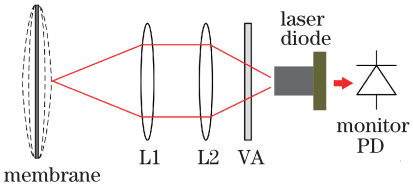

Fig. 3. Principle of infrasound detection based on the laser SM effect.

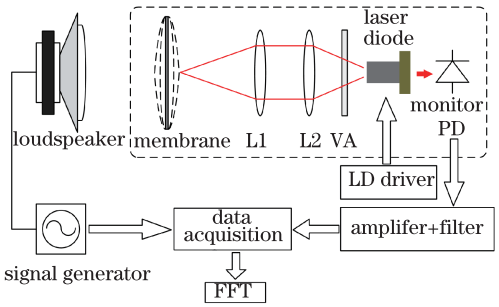

Fig. 4. Experimental setup for infrasound signal measurements.

emitting a maximum power of 5 mW at 650 nm is fed at a constant injection current of 26.6 mA. Then, the light is collimated and focused by two lenses on the membrane. A variable attenuator is used to adjust the fraction of light backreflected on the membrane surface into the LD optical cavity and keep the laser subject to moderate feedback. The intensity of the laser is monitored by the current flowing through a PD detector in the semiconductor package. The current is converted into a voltage signal by a trans-impedance preamplifier, AC coupled, amplified 1000-fold, and connected to a data acquisition board (16 bit, 1.25 MS/s). In our experiment, the sample frequency is 50 kHz ($f_s = 50$ kHz), and 200 k points ($N_s = 200$ k) are sampled in each sampling period to form a fast Fourier transform (FFT).

The sound power level (SWL) of a signal with infrasound power W_{ac} is

$$\mathrm{SWL} = 10\lg\left(\frac{W_{ac}}{W_0}\right), \tag{11}$$

where W_0 is the 0 dB reference level and equal to 10^{-12} W.

$$W_{ac} = \eta \cdot W_e = \eta\frac{U_{max}^2}{R}, \tag{12}$$

where W_e is the electrical power, η is the electro-acoustic conversion efficiency, U_{max} is the driver voltage amplitude of the speaker, and R is the nominal impedance of the speaker.

In the case of a free sound source in air at ambient temperature, the SWL is approximately related to SPL at a distance r of the source by

$$\mathrm{SPL} = \mathrm{SWL} + 10\lg\left(\frac{S_0}{4\pi r^2}\right), \tag{13}$$

where $S_0 = 1\mathrm{m}^2$.

Assuming that $\eta = 1\%$, the infrasound pressure caused by the loudspeaker vibration can then be expressed as

$$\mathrm{SPL} = 20\lg\frac{0.01U_{max}}{RP_0} + 10\lg\left(\frac{S_0}{4\pi r^2}\right). \tag{14}$$

Combining Eqs. (10) and (13) shows that the number of fringe of SM signal is proportional to the driver voltage amplitude of the speaker.

Figure 5 shows an example of a laser output waveform and the corresponding loudspeaker drive signal at 9.75 Hz. According to the shape of the SM signal, the LD is subjected to the moderate feedback regime ($1 < C < 4.6$). From the slope sequence in the sawtooth line shape (slow-fast or vice versa), the direction of the membrane motion can be determined.

The Fourier spectra of the SM signal are depicted in Fig. 6. The basic frequency is 9.75 Hz as shown in the partial enlargement figure. The frequency spectrum is composed of the basic frequency and its harmonic components consistent with the simulated result. Therefore, the infrasound frequency is the frequency of the first-order harmonic component, i.e., the first peak in the frequency spectrum. Compared with Fig. 2, the strongest peak (at 205 Hz) is approximately 21 times higher than the vibration frequency, close to the simulated result. The spectrum resolution associated with the FFT in this experiment is $f_s/N_s = 0.25$ Hz. Notably, a longer FFT used results in a higher frequency resolution.

The frequency response shown in Fig. 7 is measured by slowly sweeping a sinusoidal signal through the speaker and measuring the corresponding amplitude of the basic frequency in the Fourier spectra. The frequency values from 2 to 20 Hz can be detected.

Figure 8 shows the relationship between the number of

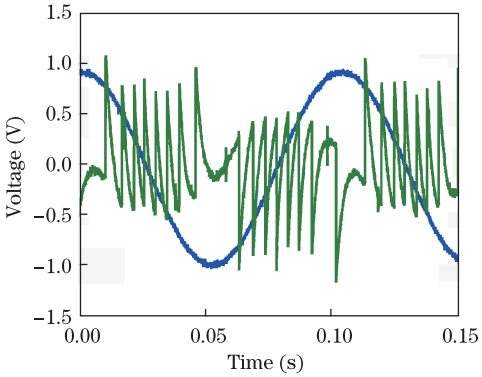

Fig. 5. (Color online) Example of a laser output waveform and the corresponding loudspeaker drive signal: loudspeaker drive signal at 9.75 Hz (blue trace) and the laser output waveform (green trace).

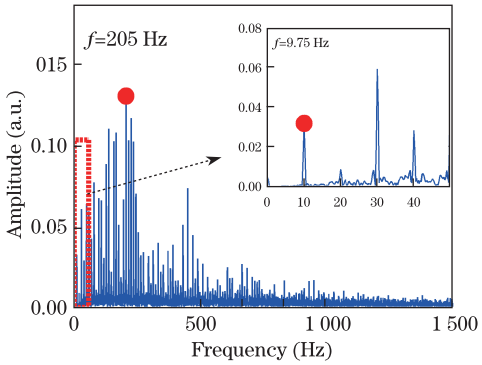

Fig. 6. (Color online) Fourier spectra of the experimental SM signal.

fringes and the amplitude of the loudspeaker drive signal $U_{\max}$. The real line is a linear fit to these data. The two variables exhibit a good linear relationship.

The minimum measureable vibration amplitude is limited by noise. The following major noise sources are found during the measurement of the SM effect: i) shot noise associated with the photodetected current; ii) interferometer phase noise caused by the finite LD linewidth; iii) mechanical noise of the optical set-up from an environmental disturbance, which generally has a $1/f$ spectrum[24]. For target distances $L_0 < 10$ m and LD linewidth below 10 MHz, the shot noise dominates over the phase noise. The ultimate sensitivity for vibration measurement is set by the quantum noise associated with the detected photocurrent signal[10,25]. This value can be expressed in terms of noise equivalent vibration as noise equivalent displacement (NED)=$[(\lambda/2\pi(S/R)]/RV$, where S/R is the SNR of the amplitude photocurrent measurement. If $S/R = 1$, then the vibrometer noise equivalent vibration is[24]

$$\Delta A_{\min} = \frac{\lambda}{2\gamma\pi}\sqrt{\frac{qFB}{2\sigma P_0}}L_0, \tag{15}$$

where q is the electron charge, σ is the net photodiode responsivity ($\sigma = 0.02$ A/W), F is the excess-noise factor (typically $F = 2$), P_0 is the power emitted by the LD, B is the measurement bandwidth, and $\gamma = 1.45 \times 10^{-4}$ m/rad, which depends on the photo lifetime and the enhancement linewidth of the LD[8].

In the moderate feedback, for an emitted $P_0 = 5$ mW, $B = 20$ Hz, and $L_0 = 0.1$ m, the minimum detectable displacement is approximately 12.7 pm·Hz$^{-1/2}$. Although this value is remarkable, other fundamental limits to the minimum detectable signal exist, including speckle statistics and thermodynamic fluctuations[25].

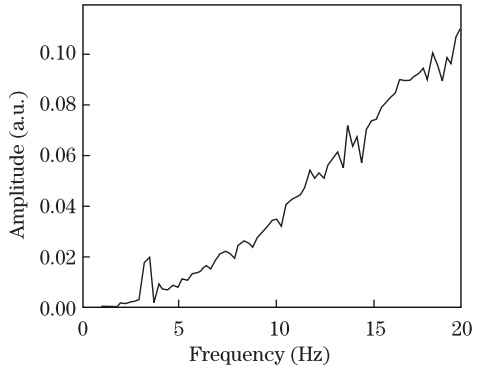

Fig. 7. Frequency response.

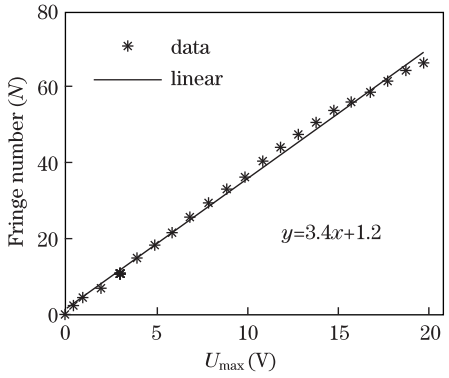

Fig. 8. Number of fringes versus the amplitude of the loudspeaker drive signal.

The proposed measuring scheme is very compact because all required components (i.e., membrane, LD, low-cost collimating lens, attenuator, and electronic circuits) can fit into a box with dimensions of a few centimeters.

In conclusion, by exploiting the SM effect under moderate feedback, a low-cost non-contact laser infrasound sensor is designed and tested. The infrasound sensor analyzes the SM signal produced in the SM-LD by the backreflected light from the vibrated aluminum membrane caused by the infrasound signal. Experimentally, infrasound signals are measured from 2 to 20 Hz with a frequency resolution of 0.25 Hz and a displacement with a resolution of $\lambda/2$. Compared currently available laser-based interferometric infrasound sensors, the proposed infrasound measurement method is simple and compact.

This work was supported by the Natural Science Foundation of Heilongjiang (No. F201105) and the research fund of Zhanjiang Normal University (No. L1106).

References

1. A. J. Bedard, Jr, and T. M. Georges, Phys. Today **53,** 32 (2000).
2. B. Alcoverro and A. Le Pichon, J. Acoust. Soc. Am. **117,** 1717 (2005).
3. D. Christie, J. Vivas Veloso, P. Campus, M. Bell, T. Hoffmann, A. Langlois, P. Martysevich, E. Demirovic, and J. Carvalho, Kerntechnik **66,** 96 (2001).
4. D. M. Donskoy and B. A. Cray, J. Acoust. Soc. Am. **129,** EL254 (2011).
5. J. S. Wilson, *Sensor Technology Handbook* (Elsevier, 2005).
6. B. Jiang, K. Yang, and J. Wang, in *Proceedings of the 2010 International Conference on Measuring Technology and Mechatronics Automation* (IEEE Computer Society, Changsha, China, 2010) p. 1049.
7. M. A. Zumberge, J. Berger, M. A. H. Hedlin, E. Husmann, S. Nooner, R. Hilt, and R. Widmer-Schnidrig, J. Acoust. Soc. Am. **113,** 2474 (2003).
8. G. Giuliani, M. Norgia, S. Donati, and T. Bosch, J. Opt. A-pure Appl. Opt. **4,** S283 (2002).
9. U. Zabit, O. D. Bernal, T. Bosch, and F. Bony, Opt. Lett. **36,** 612 (2011).
10. S. Donati, Laser Photon. Rev. **6,** 393 (2012).
11. D. Silvano, W. Zhao, and Y. Yu, Chin. Opt. (in Chinese) **5,** 93 (2012).
12. S. Ottonelli, F. De Lucia, M. Di Vietro, M. Dabbicco, G. Scamarcio, and F. P. Mezzapesa, IEEE Photon. Technol. Lett. **20,** 1360 (2008).
13. P. J. De Groot, G. M. Gallatin, and S. H. Macomber, Appl. Opt. **27,** 4475 (1988).
14. R. Lang and K. Kobayashi, IEEE J. Quantum Electron. **16,** 347 (1980).
15. K. Petermann, IEEE J. Sel. Top. Quantum **1,** 480 (1995).
16. U. Zabit, T. Bosch, and F. Bony, IEEE Sens. J. **9,** 1879 (2009).
17. S. Donati, L. Falzoni, and S. Merlo, IEEE T. Instrum. Meas. **45,** 942 (1996).
18. T. Bosch, N. Servagent, and S. Donati, Opt. Eng. **40,** 20 (2001).

19. Y. Fan, Y. Yu, J. Xi, and J. F. Chicharo, Appl. Opt. **50,** 5064 (2011).
20. C. Bes, G. Plantier, and T. Bosch, IEEE T. Instrum. Meas. **55,** 1101 (2006).
21. X. Dai, M. Wang, Y. Zhao, and J. Zhou, Opt. Express **17,** 16543 (2009).
22. X. Zhang, J. Xi, Y. Yu, and J. Chichero, in *Proceedings of the 4th IEEE International Symposium on Electronic Design, Test and Applications* 491 (2008).
23. L. E. Kinsler, A. R. Frey, and A. B. C. J. V. Sanders, *Fundamentals of Acoustics* (*4th Edn.*) (Wiley, New York, 1999).
24. G. Giuliani, S. Bozzi-Pietra, and S. Donati, Meas. Sci. Technol. **14,** 24 (2003).
25. S. Donati, *Electro-Optical Instrumentation: Sensing and Measuring with Lasers* (Prentice Hall, Upper Saddle River, NJ, 2004).